# Overall Radiation Pattern of Four Bremsstrahlung Particle System

**Mert Yücemöz**[1] **, Martin Füllekrug**[2]

[1]University of Bath
[2]University of Bath

**Key Points:**

- The total number of radiation lobes and peaks are found to be always even numbers for the particles in the same orientation.
- Every new radiation peak pair represents a new bunch of particles at the same energy level.
- Total odd numbers of radiation lobes were found to exist for the particles in different orientations.

Corresponding author: Mert Yucemoz, m.yucemoz@bath.ac.uk

**Abstract**

Terrestrial Gamma-ray Flashes exhibit slopes of ionizing radiation associated with bremsstrahlung. Bremsstrahlung has a continuous spectrum of radiation from radio waves to ionizing radiation. The Poynting vector of the emitted radiation, i.e., the radiation pattern around a single particle under the external lightning electric field during interaction with other particles or atoms, is not quite well known. The overall radiation pattern arises from the combination of radiation of parallel and perpendicular motions of a particle caused by the acceleration from the lightning electric field and the bremsstrahlung. The calculations and displays of radiation patterns are generally limited to a low-frequency approximation for radio waves and separate parallel and perpendicular motions. Here we report the radiation patterns of combined parallel and perpendicular motions from accelerated relativistic particles at low and high frequencies of the bremsstrahlung process with an external lightning electric field. The primary outcome is that radiation patterns have four relative maxima with two forward peaking and two backward peaking lobes. The asymmetry of the radiation pattern, i.e., the different intensities of forward and backward peaking lobes, are caused by the Doppler effect. A novel outcome is that bremsstrahlung has an asymmetry of the four maxima around the velocity vector caused by the curvature of the particle's trajectory as it emits radiation. This mathematical modeling helps to better understand the physical processes of a single particle's radiation pattern, which might assist the interpretation of observations with networks of radio receivers and arrays of $\gamma$-ray detectors.

## 1 Introduction

It was recently suggested that high-frequency radiation emissions observed in the atmosphere could originate from muons interacting with electric fields inside thunderclouds. This novel idea is based on a reduction of the muon detection during thunderstorm occurrences by the ground based telescope GRAPES-3 located in Ooty, India (Hariharan et al., 2019). Gamma-Ray Bursts (GRBs) are commonly thought to result from the interaction of neutron stars in outer space or comet collisions. GRBs emit photons in the energy range from keV to MeV that last ∼10 seconds. However, a ∼90 minute long GRB was detected with photon energies ∼18 GeV (Hurley et al., 1994). When Terrestrial Gamma-Ray Flashes (TGFs) were first observed by detectors of the Compton Gamma Ray Observatory (CGRO) (Fishman et al., 1994), their association with bremsstrahlung was demonstrated by the observation of the characteristic slopes of ionizing radiation (Dwyer et al., 2012a), supported by Monte Carlo simulations that included the bremsstrahlung process (Dwyer, 2007). Another example of bremsstrahlung associated with lightning discharges is the detection of ultra-low frequency (ULF) and very low frequency (VLF) radio emissions of the same electrons that are also responsible for emitting terrestrial gamma-ray flashes (Connaughton et al., 2013). TGFs are associated with low-frequency radio emissions, and these observations were used to identify their source altitude (Pu et al., 2019; Cummer et al., 2014). The source altitude was located to lie between two charged cloud layers in a thunderstorm. All the above discoveries offer experimental evidence for the continuous radiation spectrum of bremsstrahlung to occur. Relativistic runaway electrons are the source of high-frequency X- and $\gamma$-ray emissions observed in the upper troposphere at altitudes from ∼12-14 km height (Celestin, 2016). High energy relativistic electrons have a larger mean free path such that they can attain larger velocities until they collide with an atom or molecule in the atmosphere. As these electrons are capable of reaching large velocities, they can emit ionizing radiation through the bremsstrahlung process. Low energy electrons are much more likely to collide with atmospheric atoms or molecules, leading to an increase in the number of free electrons in the atmosphere (Celestin, 2016). Another working hypothesis is that bremsstrahlung radiation is emitted by thermal runaway electrons accelerated by intra-cloud lightning leader tips (Xu et al., 2015). Bremsstrahlung has a continuous electromagnetic spectrum. Low-frequency radio and optical emissions could also be due to fluorescence, where high-frequency TGFs

are absorbed by air molecules (Xu et al., 2015). Numerical Monte Carlo simulations demonstrated the significance of the bremsstrahlung process as the primary process behind high-frequency emissions (Dwyer et al., 2012b). Bremsstrahlung electrons emit radiation in forward peaking radiation patterns with an angle that scales with the inverse of the Lorentz factor of the relativistic electrons (Koch & Motz, 1959).

Asymmetric signal of $\gamma$-ray bursts measured by the Gamma-Ray Burst Monitor on the Fermi Gamma-ray Space Telescope reveal the lightning leader charge structure. Asymmetric $\gamma$-ray pulses indicate the lightning leader charge flux, which exhibits a fast rise and slow decay of the leader tip electric field (Foley et al., 2014). The asymmetries in $\gamma$-ray pulses are thought to be caused by Compton scattering (Xu et al., 2019). The rise to decay time ratio of single $\gamma$-ray pulses was measured to be approximately 0.67 (Nemiroff et al., 1994). Data from the Burst and Transient Source Experiment (BATSE) reveals two different types of spectra of $\gamma$-ray bursts known as bright and dim GRBs. It was found that dim GRBs have less photon energy than bright GRBs (Norris et al., 1994). It was observed that as time passes, overall $\gamma$-ray photons transit from bright to dim photons as a photon bunch due to a time delay of approximately 100 $\mu$s between the peaks arising from hard and soft photons (Grefenstette et al., 2008).

Experimental measurements of ionizing radiation and optical emissions by the Atmosphere Space Interactions Monitor (ASIM) on the International Space Station recently reported the detection of 217 TGFs from June 2, 2018, to April 1, 2019 (Østgaard et al., 2019), some associated with radio emissions from charged particles that are observed on the ground. All these measurements reveal the properties of $\gamma$-ray bursts. After the combination of the measurements from ground-based radio receivers and spacecraft, it was found that TGFs are produced at the very beginning of the lightning discharge process. It is well known that the observed $\gamma$-rays originate from the bremsstrahlung process (Xu et al., 2015). There are approximately $\sim 10^{17}$–$10^{19}$ Gamma-ray bursts emitted during the bremsstrahlung process. It is well known that the initially emitted ionizing radiation is not the same in terms of energy and direction compared to the radiation measured by sensors. This difference is because the emitted radiation loses energy by back-scattering and interacting with other air molecules. The interaction causes an ionization and releases more electrons, which can explain why $10^{17} - 10^{19}$ $\gamma$-rays are emitted (Dwyer, 2008). Another theory explains $\gamma$-ray bursts to originate from the large electric fields of leader tip streamers producing $\sim 10^{12}$ electrons which then increase the number of electrons within the relativistic runaway electron avalanche (RREA) process that emits $\gamma$-ray photons (Babich et al., 2014, 2015; Moss et al., 2006; Chanrion & Neubert, 2010; Celestin & Pasko, 2011; Skeltved et al., 2017).

This contribution reports the radiation interference of a four bremsstrahlung electron system from the previous modeling of an asymmetric forward peaking radiation pattern and an asymmetric backward peaking radiation pattern of a single particle bremsstrahlung process.

### 1.1 Aims & Objectives

This contribution aims to study the radiation interference of four charged bremsstrahlung particles at different energy levels. In addition, the prediction of single bremsstrahlung particle radiation patterns for different energy levels comes from the previous detailed study (Yucemoz & Füllekrug, 2020).

## 2 Radiation Interference of the Four Bremsstrahlung Electron

In order to track the radiation interference and to be able to interpret the overall radiation pattern, a system consisting of four bremsstrahlung electrons was created. The overall radiation patterns of the four bremsstrahlung electrons of different energies are presented in figure 1.

forward peaking of interfered electromagnetic radiation patterns in figure 1 is oriented in the same direction for all four particles.

As can be seen in figure 1, when all four particles are oriented in the same direction, the number of radiation lobes and the number of radiation peaks are always even numbers.

The radiation lobe refers to a single enclosed area whereas, the radiation peak refers to the maximum radiation intensity points that exist in between two minimum radiation intensity values.

During wave interference study, energy, the bremsstrahlung asymmetry, R and emitted radiation frequency have been changed. The particle's spatial initial positions and orientations of the velocity vector have been kept constant.

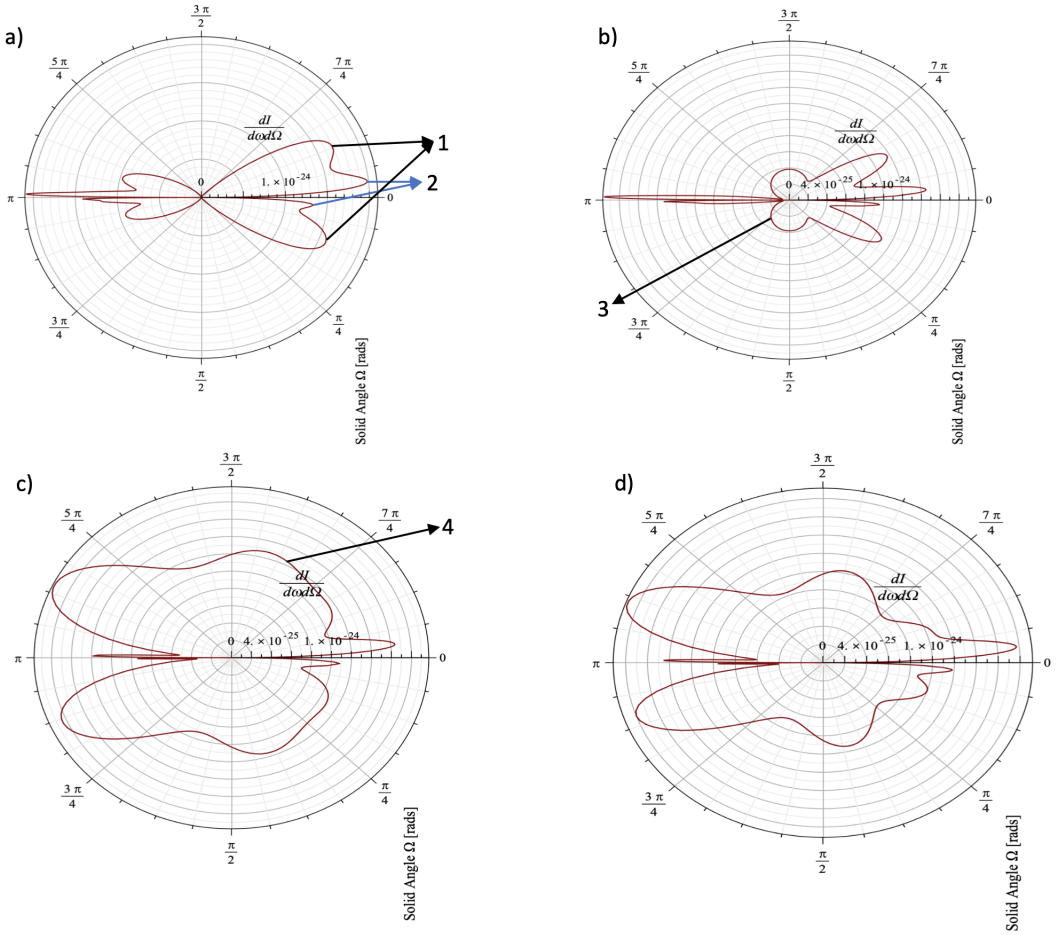


**Figure 1.** Each radiation pattern (a,b,c,d) is the interference of the radiation emitted by each four bremsstrahlung electron. The relativistic and ultra-relativistic particles are set to emit high-frequency ionizing radiation. In plot a), all four particles are high-energy relativistic particles and emits ionizing radiation. Their emitted radiation energy levels are high but not the same. Therefore, there are four different radiation peaks in the forward direction. Each pair of peaks indicated with one and two represents a certain group of particles emitting energy at similar levels. In plot b) one particle is high energy ultra-relativistic, one particle is non-relativistic, and the other two particles are medium energy relativistic particles. At low-energy relativistic speed, the dipole radiation pattern collapses to form the initial stages of the forward-backward radiation pattern. The peak at point three is the outcome of the interference of radiation from non-relativistic and medium energy relativistic particles. In plot c) two of the particles are non-relativistic, one particle is medium energy relativistic particle and one particle is high energy relativistic particle. In plot d) one particle is non-relativistic, two particles are medium energy relativistic particles and one particle is high energy relativistic particle.

## 3 Radiation Interference of the Four Bremsstrahlung Electron Approaching and Radiating at Different Orientations

In this section, during wave interference study, only particles orientation, energy, the bremsstrahlung asymmetry, R, and emitted radiation frequency have been changed. The particle's spatial initial position has been kept constant.

Different orientations mean differences in the orientation of the particle's velocity vector.

Besides bremsstrahlung asymmetry (R), orientations above $\pi$ radians should not change the shape of the overall radiation pattern due to the symmetry in the angular direction of the radiation patterns.

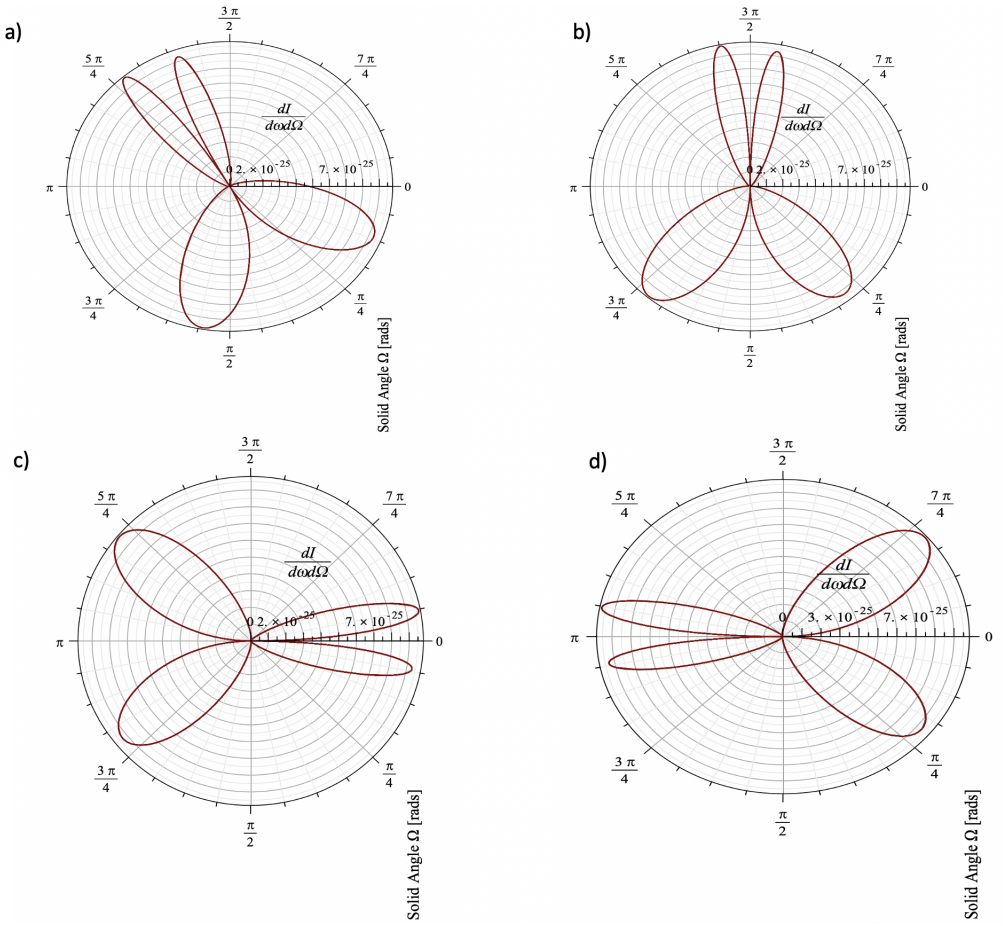


**Figure 2.** During the bremsstrahlung process particles randomly follow curved trajectories and emit radiation at different orientations. Therefore, expected radiation patterns can be at random orientations, and emitted electromagnetic waves can interfere with each other at these random orientations.

Independent of the radiation pattern of different particle velocities, radiation is highly in phase closer to the particle (i.e center of the radiation pattern where all radiation lobes start and end). As this region is the most common in phase region of all radiation patterns, it is the most sensitive region to destructive interference at the right orientation angles for all particles in a multi-particle system.

Therefore, as displayed in figure 3, at right orientation angles for each particle in the multi-particle system (table 2). The radiation intensity closer to the particle located at the origin of the graph in all figures is zero. This produces an overall radiation pattern that looks like radiation is not emanated from the particle, as there is no radiation pattern connecting with the particle located in the origin, figure 3b.

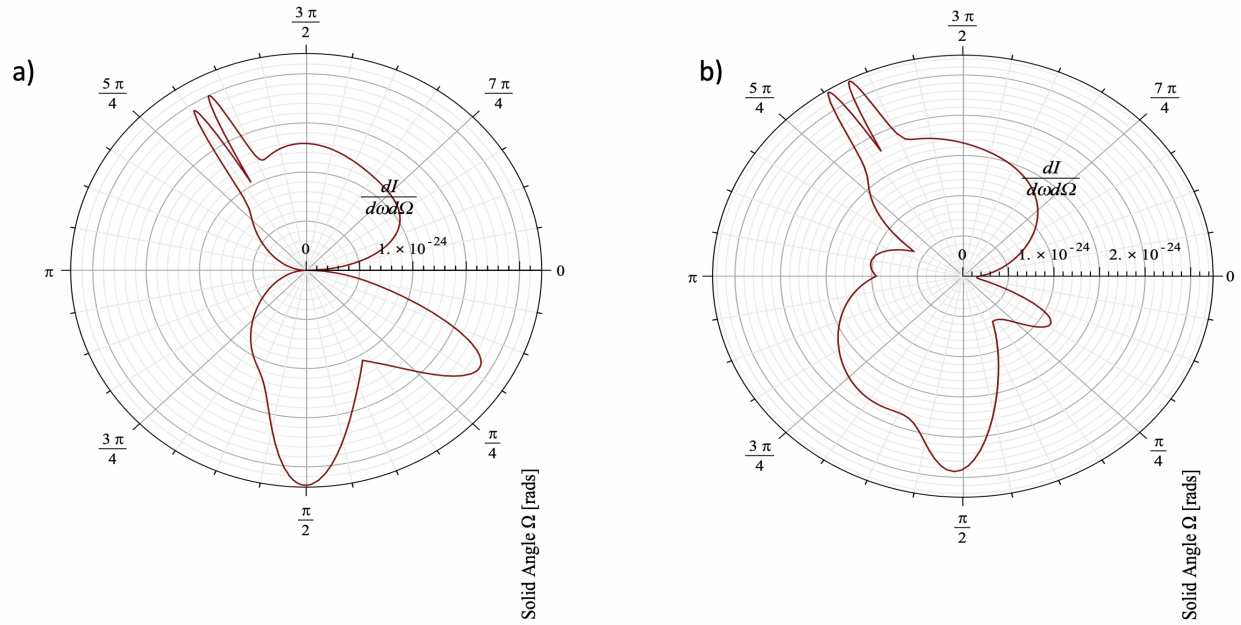


**Figure 3.** Theoretically, an observer very close to particle emitting radiation of any pattern from dipole to forward-backward peaking, would not be able to distinguish and tell the type (Relativistic or non-relativistic) of the radiation pattern. This can be observed by comparing non-relativistic, dipole, and relativistic, forward-backward peaking radiation patterns at the origin where the particle is located. In this region close to the particle at origin, emitted radiation intensity, hence frequency are very close to each other independent of the type of radiation pattern. As this is a common region for all radiation patterns where they share the same physical properties (frequency, amplitude), at the right orientation angle, complete destructive wave interference is more likely to occur. Complete rather than partial destructive wave interference is because of the same frequency match specific to this region. Therefore, this results in a radiation pattern given in 3b, where the radiation pattern connecting to the particle at the origin disappears due to destructive wave interference. Hence, the overall interfered radiation pattern emitted by the four-particle at different orientations but on the same spatial position at origin seems to be not emanated from the particle as there is no radiation pattern connecting to the particles at the origin (Figure 3b).

It would be expected for all types of radiation patterns emanated from the accelerated particle to be similar close to the particle where they are emitted. This is because parts of the radiation pattern close to the particle at origin are the start of the radia-

tion process. As the radiation changes temporally and as the bremsstrahlung is a continuous spectrum of radiation, at the beginning of the radiation process closer to the particle at origin, where the time is close to zero, there would be not enough temporal variation in the radiation pattern. The radiation pattern requires time to change and at the early stage of the emission, the time is at its beginning. Hence, radiation patterns should share a similarity closer to the particle at the origin independent of the type of the pattern. Therefore, an observer closer to the particle should not be able to distinguish the type of radiation pattern (i.e. relativistic or non-relativistic radiation patterns).

| *Speed and emitted radiation frequency of the four particle for overall radiation pattern, a in figure 3.* | | | | |
|---|---|---|---|---|
| Particle (Electron) | Scaled Bremsstrahlung Electron Velocity $\beta$ (Dimensionless) | Emitted Radiation Frequency ($Hz$) | Bremsstrahlung Asymmetry, R | Orientation angle, rads |
| Particle 1 | 0.67 | 3 MHz | $\frac{1}{3}$ | - |
| Particle 2 | 0.01 | 5 kHz | $\frac{1}{9}$ | - |
| Particle 3 | 0.93 | 80 MHz | $\frac{1}{8}$ | $\frac{\pi}{3}$-$\theta_{n\beta}$ |
| Particle 4 | 0.89 | 9 MHz | $\frac{1}{6}$ | $\pi$-$\theta_{n\beta}$ |

**Table 1.** Input parameters for figure 3a

| *Speed and emitted radiation frequency of the four particle for overall radiation pattern, b in figure 3.* | | | | |
|---|---|---|---|---|
| Particle (Electron) | Scaled Bremsstrahlung Electron Velocity $\beta$ (Dimensionless) | Emitted Radiation Frequency ($Hz$) | Bremsstrahlung Asymmetry, R | Orientation angle, rads |
| Particle 1 | 0.67 | 3 MHz | $\frac{1}{3}$ | - |
| Particle 2 | 0.01 | 5 MHz | $\frac{1}{9}$ | - |
| Particle 3 | 0.93 | 80 MHz | $\frac{1}{8}$ | $\frac{\pi}{3}$-$\theta_{n\beta}$ |
| Particle 4 | 0.89 | 9 MHz | $\frac{1}{6}$ | $\frac{\pi}{6}$-$\theta_{n\beta}$ |

**Table 2.** Input parameters for figure 3b

**Acknowledgments**

I would like to thank my supervisor Dr.Martin Füllekrug for all the opportunities, suggestions, guidance, reviews, and support throughout my first and second years of PhD. EPSRC and MetOffice sponsor my PhD project under contract numbers EG-EE1239 and EG-EE1077. MF acknowledge support from the Natural Environment Research Council (NERC) for under grants NE/L012669/1 and NE/H024921/1. MY wishes to thank Dr. Adrian Hill for mathematical support in helping me solve integral with a divergence problem and my family for their support and good wishes. The Maple worksheets used to simulate the particle trajectory, external lightning leader tip electric field, particle velocity, and the radiation patterns are openly available from the University of Bath Research Data Archive at https://doi.org/10.15125/BATH-00810.

## References

Babich, L. P., Bochkov, E. I., & Kutsyk, I. M. (2014). Mechanism of generation of runaway electrons in a lightning leader. *JETP Letters*, *99*(7), 386–390. Retrieved from `https://doi.org/10.1134/S0021364014070029` doi: 10.1134/S0021364014070029

Babich, L. P., Bochkov, E. I., Kutsyk, I. M., Neubert, T., & Chanrion, O. (2015). A model for electric field enhancement in lightning leader tips to levels allowing X-ray and $\gamma$ ray emissions. *Journal of Geophysical Research: Space Physics*, *120*(6), 5087-5100. Retrieved from `https://agupubs.onlinelibrary.wiley.com/doi/abs/10.1002/2014JA020923` doi: 10.1002/2014JA020923

Celestin, S. (2016, December). Electron acceleration mechanisms in thunderstorms. *arXiv*, 1-6. doi: arXiv:1701.00105[astro-ph.HE]

Celestin, S., & Pasko, V. P. (2011). Energy and fluxes of thermal runaway electrons produced by exponential growth of streamers during the stepping of lightning leaders and in transient luminous events. *Journal of Geophysical Research: Space Physics*, *116*(A3). Retrieved from `https://agupubs.onlinelibrary.wiley.com/doi/abs/10.1029/2010JA016260` doi: 10.1029/2010JA016260

Chanrion, O., & Neubert, T. (2010). Production of runaway electrons by negative streamer discharges. *Journal of Geophysical Research: Space Physics*, *115*(A6), 1-10. Retrieved from `https://agupubs.onlinelibrary.wiley.com/doi/abs/10.1029/2009JA014774` doi: 10.1029/2009JA014774

Connaughton, V., Briggs, M. S., Xiong, S., Dwyer, J. R., Hutchins, M. L., Grove, J. E., ... Wilson-Hodge, C. (2013, May). Radio signals from electron beams in terrestrial gamma ray flashes. *Journal of Geophysical Research: Space Physics*, *118*(5), 2313-2320. Retrieved from `https://agupubs.onlinelibrary.wiley.com/doi/abs/10.1029/2012JA018288` doi: 10.1029/2012JA018288

Cummer, S. A., Briggs, M. S., Dwyer, J. R., Xiong, S., Connaughton, V., Fishman, G. J., ... Solanki, R. (2014, December). The source altitude, electric current, and intrinsic brightness of terrestrial gamma ray flashes. *Geophysical Research Letters*, *41*(23), 8586-8593. Retrieved from `https://agupubs.onlinelibrary.wiley.com/doi/abs/10.1002/2014GL062196` doi: 10.1002/2014GL062196

Dwyer, J. R. (2007). Relativistic breakdown in planetary atmospheres. *Physics of Plasmas*, *14*(4), 042901. Retrieved from `https://doi.org/10.1063/1.2709652` doi: 10.1063/1.2709652

Dwyer, J. R. (2008). Source mechanisms of terrestrial gamma-ray flashes. *Journal of Geophysical Research: Atmospheres*, *113*(D10), 1-12. Retrieved from `https://agupubs.onlinelibrary.wiley.com/doi/abs/10.1029/2007JD009248` doi: 10.1029/2007JD009248

Dwyer, J. R., Smith, D. M., & Cummer, S. A. (2012a). High-energy atmospheric physics: Terrestrial gamma-ray flashes and related phenomena. *Space Science*

*Reviews*, *173*(1), 133–196. Retrieved from https://doi.org/10.1007/s11214-012-9894-0 doi: 10.1007/s11214-012-9894-0

Dwyer, J. R., Smith, D. M., & Cummer, S. A. (2012b, June). High-Energy Atmospheric Physics: Terrestrial Gamma-Ray Flashes and Related Phenomena. *Space Science Reviews*, *173*(1), 133–196. Retrieved from https://doi.org/10.1007/s11214-012-9894-0 doi: 10.1007/s11214-012-9894-0

Fishman, G. J., Bhat, P. N., Mallozzi, R., Horack, J. M., Koshut, T., Kouveliotou, C., ... Christian, H. J. (1994). Discovery of intense gamma-ray flashes of atmospheric origin. *Science*, *264*(5163), 1313–1316. Retrieved from https://science.sciencemag.org/content/264/5163/1313 doi: 10.1126/science.264.5163.1313

Foley, S., Fitzpatrick, G., Briggs, M. S., Connaughton, V., Tierney, D., McBreen, S., ... Wilson-Hodge, C. (2014, June). Pulse properties of terrestrial gamma-ray flashes detected by the Fermi Gamma-Ray Burst Monitor. *Journal of Geophysical Research: Space Physics*, *119*(7), 5931-5942. Retrieved from https://agupubs.onlinelibrary.wiley.com/doi/abs/10.1002/2014JA019805 doi: 10.1002/2014JA019805

Grefenstette, B. W., Smith, D. M., Dwyer, J. R., & Fishman, G. J. (2008, March). Time evolution of terrestrial gamma ray flashes. *Geophysical Research Letters*, *35*(6), 1-5. Retrieved from https://agupubs.onlinelibrary.wiley.com/doi/abs/10.1029/2007GL032922 doi: 10.1029/2007GL032922

Hariharan, B., Chandra, A., Dugad, S. R., Gupta, S. K., Jagadeesan, P., Jain, A., ... Tanaka, K. (2019, Mar). Measurement of the electrical properties of a thundercloud through muon imaging by the grapes-3 experiment. *Phys. Rev. Lett.*, *122*, 105101. Retrieved from https://link.aps.org/doi/10.1103/PhysRevLett.122.105101 doi: 10.1103/PhysRevLett.122.105101

Hurley, K., Dingus, B. L., Mukherjee, R., Sreekumar, P., Kouveliotou, C., Meegan, C., ... Niel, M. (1994, December). Detection of a γ-ray burst of very long duration and very high energy. *Nature*, *372*(6507), 652–654. Retrieved from https://doi.org/10.1038/372652a0 doi: 10.1038/372652a0

Koch, H. W., & Motz, J. W. (1959, Oct). Bremsstrahlung cross-section formulas and related data. *Rev. Mod. Phys.*, *31*, 920–955. Retrieved from https://link.aps.org/doi/10.1103/RevModPhys.31.920 doi: 10.1103/RevModPhys.31.920

Moss, G. D., Pasko, V. P., Liu, N., & Veronis, G. (2006). Monte Carlo model for analysis of thermal runaway electrons in streamer tips in transient luminous events and streamer zones of lightning leaders. *Journal of Geophysical Research: Space Physics*, *111*(A2), 1-37. Retrieved from https://agupubs.onlinelibrary.wiley.com/doi/abs/10.1029/2005JA011350 doi: 10.1029/2005JA011350

Nemiroff, R. J., Norris, J. P., Kouveliotou, C., Fishman, G. J., Meegan, C. A., & Paciesas, W. S. (1994, March). Gamma-Ray Bursts Are Time-asymmetric. *Astrophysical Journal*, *423*, 432-435. doi: 10.1086/173819

Norris, J. P., Nemiroff, R. J., Bonnell, J. T., Wickramasinghe, W. A. D. T., Kouveliotou, C., Paciesas, W. S., ... Meegan, C. A. (1994, November). Gross Spectral Differences between Bright and DIM Gamma-Ray Bursts. *Astrophysical Journal Letters*, *435*, L133. doi: 10.1086/187612

Pu, Y., Cummer, S. A., Lyu, F., Briggs, M., Mailyan, B., Stanbro, M., & Roberts, O. (2019, June). Low Frequency Radio Pulses Produced by Terrestrial Gamma-Ray Flashes. *Geophysical Research Letters*, *46*(12), 6990-6997. Retrieved from https://agupubs.onlinelibrary.wiley.com/doi/abs/10.1029/2019GL082743 doi: 10.1029/2019GL082743

Skeltved, A. B., Østgaard, N., Mezentsev, A., Lehtinen, N., & Carlson, B. (2017). Constraints to do realistic modeling of the electric field ahead of the tip of a lightning leader. *Journal of Geophysical Research: Atmospheres*, *122*(15),

8120-8134. Retrieved from https://agupubs.onlinelibrary.wiley.com/doi/abs/10.1002/2016JD026206 doi: 10.1002/2016JD026206

Xu, W., Celestin, S., & Pasko, V. P. (2015, January). Optical emissions associated with terrestrial gamma ray flashes. *Journal of Geophysical Research: Space Physics*, *120*(2), 1355-1370. Retrieved from https://agupubs.onlinelibrary.wiley.com/doi/abs/10.1002/2014JA020425 doi: 10.1002/2014JA020425

Xu, W., Celestin, S., Pasko, V. P., & Marshall, R. A. (2019, August). Compton Scattering Effects on the Spectral and Temporal Properties of Terrestrial Gamma-Ray Flashes. *Journal of Geophysical Research: Space Physics*, *124*(8), 7220-7230. Retrieved from https://agupubs.onlinelibrary.wiley.com/doi/abs/10.1029/2019JA026941 doi: 10.1029/2019JA026941

Yucemoz, M., & Füllekrug, M. (2020). Asymmetric backward peaking radiation pattern from a relativistic particle accelerated by lightning leader tip electric field. *Earth and Space Science Open Archive*, 28. Retrieved from https://doi.org/10.1002/essoar.10503599.1 doi: 10.1002/essoar.10503599.1

Østgaard, N., Neubert, T., Reglero, V., Ullaland, K., Yang, S., Genov, G., ... Al-nussirat, S. (2019, December). First 10 Months of TGF Observations by ASIM. *Journal of Geophysical Research: Atmospheres*, *124*(24), 14024-14036. Retrieved from https://agupubs.onlinelibrary.wiley.com/doi/abs/10.1029/2019JD031214 doi: 10.1029/2019JD031214